Supplementary Information (SI) for Physical Chemistry Chemical Physics.

Supporting information for:

Molecular Simulations of ssDNA/ssRNA in [BMIM][PF_6] Ionic Liquid: A Novel Biopolymer Electrolyte for Rechargeable Battery Applications

Akash K. Meel and Santosh Mogurampelly*

Polymer Electrolytes and Materials Group (PEMG), Department of Physics, Indian Institute of Technology Jodhpur, Rajasthan, India-342030

Abstract

The supplementary document contains (S1) System details, including the molecular composition of each system, equilibrium density, and MD snapshots. (S1.1) Force field parameters for ionic liquid. (S1.2) System assembly procedure. (S2) Diffusion coefficient calculation methodology. (S3) Stress autocorrelation function.

1 System Details

The snapshots of the simulated systems after 1.1 μs, visualized using VMD, are presented in Figure 1.[1] These images illustrate the distribution of ionic species around the polymer chains, confirming the uniform incorporation of ssDNA/ssRNA within the ionic liquid environment. This observation aligns with our density profile and radial distribution function analyses, which indicate that the ions are distributed homogeneously throughout the system and that the fundamental liquid structure of [BMIM][PF_6] remains intact despite the presence of biopolymers.

Table 1 provides an overview of the key parameters of the simulated systems, including the simulation box volume, density, molecular composition, and total number of atoms. Each polymer-containing system consists of 10 polymer chains, with each chain comprising 12 monomers, which comes out to be an approximate polymer loading of 20%. This composition was selected to ensure a balance between computational efficiency and system size, allowing for the accurate capture of ion-polymer interactions over extended simulation timescales. The equilibrium density of neatIL was determined to be 1321.46 kg/m^3, closely matching the experimental value of 1314.55 kg/m^3 for [BMIM][PF_6] reported by Tokuda et al.[2] Notably, the incorporation of ssDNA leads to a slight increase in system density compared to neatIL.

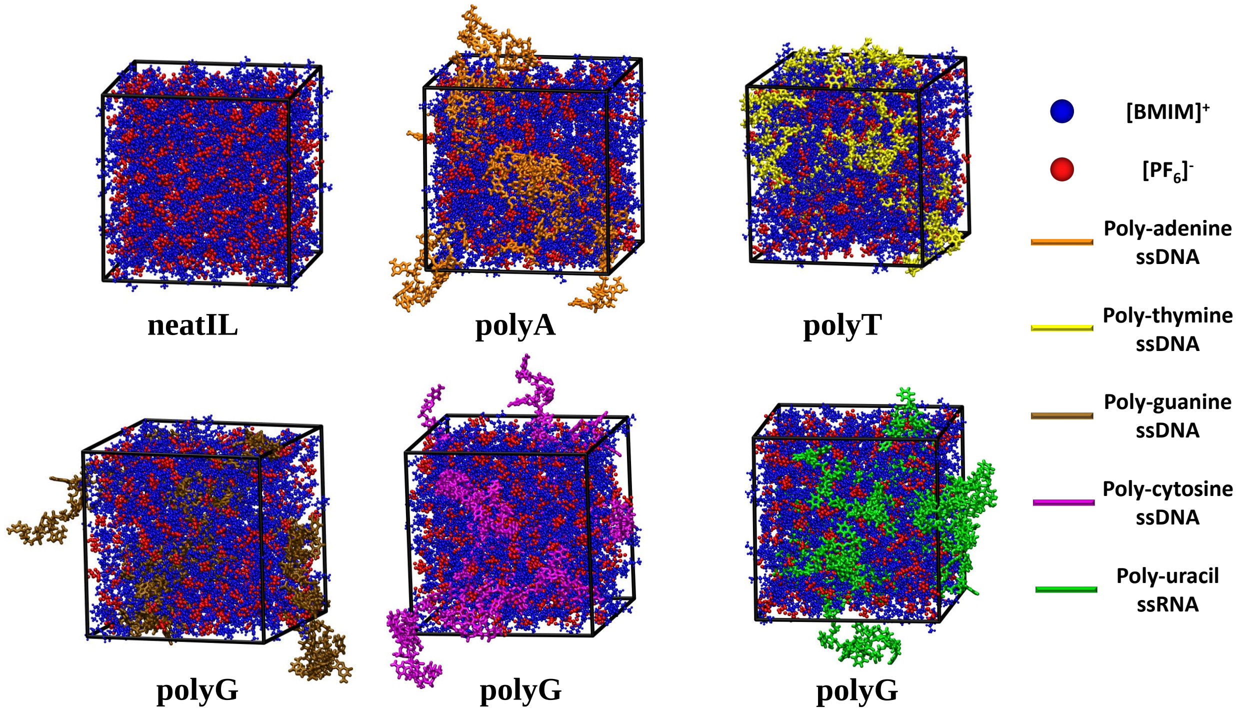

Figure 1 Molecular dynamics simulation snapshots of different systems, including neat IL and ssDNA/ssRNA homopolymers in neat IL.

Table 1 Key parameters of the simulated systems after 1.1 μs, including simulation box volume, density, temperature, number of molecules of each species, and total atom count.

System	V (nm^3)	ρ (kg m^{-3})	T (K)	BMIM$^+$	PF$_6^-$	Polymer Chains	Total Atoms
neatIL	182.57	1321.46	363	512	512	0	16,384
polyA	198.67	1347.29	363	512	362	10	19,174
polyT	198.72	1335.09	363	512	362	10	19,174
polyG	198.83	1357.43	363	512	362	10	19,294
polyC	195.44	1342.09	363	512	362	10	18,934
polyU	197.54	1353.07	363	512	362	10	18,934

1.1 Force Field Parameters

In our simulations, we employed a modified OPLS-AA force field to model the ionic liquid [BMIM][PF$_6$], using a charge scaling factor of 0.8e as proposed by Bhargava and Subramanian.[3] The bonded and nonbonded parameters for the BMIM$^+$ cation and PF$_6^-$ anion used in our simulations are provided below and are directly adapted from the GROMACS-compatible `.itp` files based on the aforementioned modifications. For the nucleic acid components, we used the OL15 force field for ssDNA and the OL3 force field for ssRNA, both of which are widely validated and specifically optimized for nucleic acid conformational behavior. Since these are standard, well-established force fields applied without further modifications, we do not list their parameters here. Researchers interested in the OL15 and OL3 force fields may refer to the original publications and their corresponding AMBER parameter files for complete details.[4,5] The complete bonded and nonbonded parameters used for the [BMIM][PF$_6$] ionic liquid in our study are listed below.

Table 2 Nonbonded parameters for atoms of $[\mathrm{BMIM}]^+$ and $[\mathrm{PF}_6]^-$

atomtype	mass (a.m.u)	charge (e)	σ (nm)	ε (kJ/mol)
CR	12.011	0.060	0.355	0.29289
NA1	14.007	0.052	0.325	0.71131
NA2	14.007	0.052	0.325	0.71131
CW1	12.011	-0.020	0.355	0.29289
CW2	12.011	-0.020	0.355	0.29289
HR	1.008	0.096	0.172	0.12553
HW1	1.008	0.096	0.172	0.12553
HW2	1.008	0.096	0.172	0.12553
CM	12.011	-0.089	0.350	0.27615
HM	1.008	0.105	0.192	0.12553
CA	12.011	-0.089	0.350	0.27615
HA	1.008	0.105	0.192	0.12553
CS1	12.011	-0.038	0.350	0.27615
CS2	12.011	-0.038	0.350	0.27615
HS1	1.008	0.026	0.250	0.12553
HS2	1.008	0.026	0.250	0.12553
CT	12.011	-0.065	0.350	0.27615
HT	1.008	0.026	0.250	0.12553
P	30.974	0.580	0.394	0.83680
F	18.998	-0.230	0.311	0.25520

Table 3 Bond parameters for $[\mathrm{BMIM}]^+$ and $[\mathrm{PF}_6]^-$. The *function* definitions can be found in the GROMACS manual (Chapter 5, Section 5.6.6, Table 5.14).

Pair	function	c_0 (nm)	c_1 (kJ.mol^{-}1.nm^{-}2)
NA2-CR	1	0.1335	462238.2
NA2-CW2	1	0.1384	341779.2
NA2-CA	1	0.1478	240423.5
NA1-CR	1	0.1385	388624.1
NA1-CW1	1	0.1386	343366.6
NA1-CM	1	0.1486	229441.3
CR-HR	1	0.1074	335727.5
CW2-HW2	1	0.1079	330918.4
CW2-CW1	1	0.1352	444779.2
CW1-HW1	1	0.1081	331703.3
CM-HM	1	0.1083	304303.1

Pair	**function**	**c_0 (nm)**	**c_1 (kJ.mol^{-}1.nm^{-}2)**
CA-HA	1	0.1092	299342.6
CA-CS1	1	0.1534	234437.0
CS1-HS1	1	0.1091	290782.9
CS1-CS2	1	0.1536	235571.7
CS2-HS2	1	0.1095	292126.8
CS2-CT	1	0.1532	240677.0
CT-HT	1	0.1093	294369.5
P-F	1	0.1596	418400.0

Table 4 Angle parameters for $[\mathrm{BMIM}]^+$ and $[\mathrm{PF}_6]^-$. The *function* definitions can be found in the GROMACS manual (Chapter 5, Section 5.6.6, Table 5.14).

Triplet	**function**	**c_0 (deg)**	**c_1 (kJ.mol^{-}1.rad^{-}2)**
NA2-CR-NA1	1	109.164	2114.96
NA2-CR-HR	1	125.132	552.97
NA2-CW2-HW2	1	122.991	517.29
NA2-CW2-CW1	1	107.291	2245.15
NA2-CA-HA	1	106.307	600.89
NA2-CA-CS1	1	112.124	659.64
NA1-CR-HR	1	125.669	540.71
NA1-CW1-CW2	1	106.709	2135.27
NA1-CW1-HW1	1	122.790	571.58
NA1-CM-HM	1	104.182	684.29
CW2-NA2-CR	1	108.165	813.74
CW2-CW1-HW1	1	130.162	490.59
CW1-NA1-CR	1	107.813	2231.95
CW1-CW2-HW2	1	130.027	541.58
CM-NA1-CR	1	126.384	758.85
CM-NA1-CW1	1	125.886	814.82
HM-CM-HM	1	109.80	276.14
CA-NA2-CR	1	126.178	707.88
CA-NA2-CW2	1	126.334	739.62
CA-CS1-HS1	1	109.146	562.39
CA-CS1-CS2	1	112.443	677.29
HA-CA-HA	1	107.853	527.29
HA-CA-CS1	1	111.966	527.46
CS1-CS2-HS2	1	107.908	497.56

Triplet	function	c_0 (deg)	c_1 (kJ.mol^{-1}.rad^{-2})
CS1-CS2-CT	1	114.212	672.78
HS1-CS1-HS1	1	107.458	473.31
CS2-CS1-HS1	1	108.941	462.07
CS2-CT-HT	1	111.352	535.35
HS2-CS2-HS2	1	106.005	686.97
CT-CS2-HS2	1	109.477	492.74
HT-CT-HT	1	108.358	571.82
F-P-F	1	90.000	627.6

Table 5 Dihedral parameters for [BMIM]$^+$. The *function* definitions can be found in the GROMACS manual (Chapter 5, Section 5.6.6, Table 5.14).

Quadruplet	function	c_0 (kJ.mol^{-1})	c_1 (kJ.mol^{-1})	c_2 (kJ.mol^{-1})	c_3 (kJ.mol^{-1})
NA1-CW1-CW2-NA2	5	0.000	89.956	0.000	0.000
NA2-CW2-CW1-HW1	5	0.000	89.956	0.000	0.000
NA2-CA-CS1-HS1	5	0.000	0.000	0.000	0.000
NA2-CA-CS1-CS2	5	-14.962	6.326	-2.409	0.000
CR-NA2-CW2-HW2	5	0.000	25.104	0.000	0.000
CR-NA2-CW2-CW1	5	0.000	25.104	0.000	0.000
CR-NA2-CA-HA	5	0.000	0.000	0.000	0.000
CR-NA2-CA-CS1	5	-13.882	-4.644	-3.138	0.000
CR-NA1-CW1-CW2	5	0.000	25.104	0.000	0.000
CR-NA1-CW1-HW1	5	0.000	25.104	0.000	0.000
CR-NA1-CM-HM	5	0.000	0.000	0.000	0.000
CW2-NA2-CR-NA1	5	0.000	38.919	0.000	0.000
CW2-NA2-CA-HA	5	-11.715	-22.175	1.464	0.000
CW2-NA2-CA-CS2	5	-15.983	-12.552	2.426	0.000
HW2-CW2-CW1-NA1	5	0.000	89.956	0.000	0.000
HW1-CW1-CW2-HW2	5	0.000	89.956	0.000	0.000
CW1-NA1-CR-NA2	5	0.000	38.919	0.000	0.000
CW1-NA1-CR-HR	5	0.000	38.919	0.000	0.000
CW1-NA1-CM-HM	5	0.000	0.000	1.037	0.000
CM-NA1-CR-NA2	5	0.000	38.919	0.000	0.000
CM-NA1-CR-HR	5	0.000	38.919	0.000	0.000
CM-NA1-CW1-CW2	5	0.000	25.104	0.000	0.000
CM-NA1-CW1-HW1	5	0.000	25.104	0.000	0.000
CA-NA2-CR-NA1	5	0.000	38.919	0.000	0.000

Quadruplet	function	c_0 (kJ.mol^{-}1)	c_1 (kJ.mol^{-}1)	c_2 (kJ.mol^{-}1)	c_3 (kJ.mol^{-}1)
CA-NA2-CR-HR	5	0.000	38.919	0.000	0.000
CA-NA2-CW2-HW2	5	0.000	25.104	0.000	0.000
CA-NA2-CW2-CW1	5	0.000	25.104	0.000	0.000
CA-CS1-CS2-HS2	5	0.000	0.000	3.063	0.000
CA-CS1-CS2-CT	5	10.878	-0.418	1.674	0.000
HA-CA-CS1-HS1	5	0.000	-0.628	2.661	0.000
HA-CA-CS1-CS2	5	0.000	0.000	3.063	0.000
CS1-CS2-CT-HT	5	0.000	0.000	3.063	0.000
HS1-CS1-CS2-HS2	5	0.000	0.000	2.661	0.000
HS1-CS1-CS2-CT	5	0.000	0.000	3.062	0.000
HS2-CS2-CT-HT	5	0.000	0.000	2.661	0.000
CM-NA-CR-CW improper	5	0.000	8.368	0.000	0.000
CA-NA-CR-CW improper	5	0.000	8.368	0.000	0.000
HW-CW-NA-CW improper	5	0.000	9.205	0.000	0.000
HW-CW-NA-CW improper	5	0.000	9.205	0.000	0.000
HR-CR-NA-NA improper	5	0.000	9.205	0.000	0.000

1.2 System Assmbely

The systems simulated in this work were constructed using a combination of tools including `tleap` (from the AmberTools package), `acpype`, and `PACKMOL`. Below is a detailed step-by-step procedure to generate the initial `.gro` files, which serve as the starting point for molecular dynamics simulations (i.e., from energy minimization to production runs):

i. Obtain the [BMIM]$^+$ and [PF$_6$]$^-$ ion structures in `.pdb` format from the OPLS-AA parameter repository[6].

ii. Construct the single-stranded DNA (ssDNA) or RNA (ssRNA) homopolymer structures using the `tleap` module from AmberTools.[7] For ssDNA, load the `OL15` force field; for ssRNA, load `OL3`. Define the desired sequence using the `sequence` command. For example, `ssdna = sequence { DA DA DA DA DA DA DA DA DA DA DA DA }` creates a 12-mer polyA chain. Save the resulting structure in `.pdb` format, along with the corresponding `.prmtop` and `.inpcrd` topology files.

iii. Generate the initial configuration using `PACKMOL` by randomly placing the required number of each molecular species into a simulation box with sufficient dimensions to avoid atomic overlaps.[8]

iv. Convert the `.pdb` output from `PACKMOL` into GROMACS-compatible `.gro` format using the `gmx editconf` utility.

v. Use `acpype` to convert the `.prmtop` and `.inpcrd` files generated by `tleap` into GROMACS-compatible `.itp` files. Perform this step for each distinct ssDNA or ssRNA molecule type.[9]

vi. The `.itp` files for ions can be generated using the OPLS-AA parameters described in Section 1.1.

vii. Create a system-specific topology file (`.top`) that includes all relevant `.itp` files and defines the number of molecules of each type present in the simulation box (as detailed in Table 1).

viii. Once both the input `.gro` and corresponding `.top` files are ready, initiate molecular dynamics simulations using standard GROMACS workflows: starting with energy minimization, followed by NVT and NPT equilibration, and concluding with production MD.

2 Diffusion Coefficient Calculation Methodology

To accurately compute the self-diffusion coefficients of ions, we employed a block-based analysis to ensure that only the regions exhibiting normal diffusion were considered. To this effect, the MSD data were divided into overlapping blocks of 10 ns duration. Specifically, the first block was constructed using MSD values from 0 ps to 10 ns. The next block was defined starting at 1 ps, incorporating MSD values from 1 ps to 10.001 ns, and so on. This procedure was continued for all possible starting points, ensuring a comprehensive sampling of diffusion behavior over time. For each block, the MSD data was fitted to a power-law function of the form $MSD(t) \sim t^{\beta}$, where the exponent β quantifies deviations from ideal diffusion. Blocks in which the fitted exponent satisfied $0.95 < \beta < 1.05$ were selected to ensure that only diffusive regions were included in the calculation. The average diffusion coefficient for each ion type can then be calculated using:

$$D = \frac{1}{N_{\text{blocks}}} \sum_{i=1}^{N_{\text{blocks}}} \frac{1}{6} \frac{d}{dt} \text{MSD}_i(t).$$

where the slope $\frac{d}{dt}MSD(t)$ is obtained by fitting a straight line through the MSD data of the chosen block. The data presented in Table 6 provides insights into the behavior of MSD with time for the different simulated systems. The column labeled "Number of Blocks" represents the number of 10 ns blocks that met the criterion $0.95 < \beta < 1.05$ within the total 1.1 μs trajectory. A larger number of valid blocks indicates that the system transitions to the diffusive regime quickly and remains there for longer durations. For neatIL, we observe the highest number of valid blocks which is consistent with earlier discussions. In contrast, polymer-containing systems show a significant reduction in valid blocks, indicating prolonged subdiffusive behavior due to polymer-ion interactions.

System	**BMIM$^+$**			**PF$_6^-$**		
	# Blocks Used	β_{avg}	β_{std}	# Blocks Used	β_{avg}	β_{std}
NeatIL	41414	0.986	0.014	47046	0.996	0.017
PolyA	81	0.995	0.032	244	0.983	0.031
PolyT	4562	0.981	0.025	1008	0.998	0.026
PolyG	3995	0.970	0.017	1586	0.970	0.020
PolyC	767	0.958	0.007	548	0.965	0.015
PolyU	1007	0.968	0.012	1530	0.994	0.034

Table 6 Block averaging analysis of ion transport in different simulated systems. The table lists the number of blocks used for statistical averaging (# Blocks Used) and the corresponding average scaling exponent (β_{avg}) with its standard deviation (β_{std}) for cations and anions in each system.

3 Stress autocorrelation function

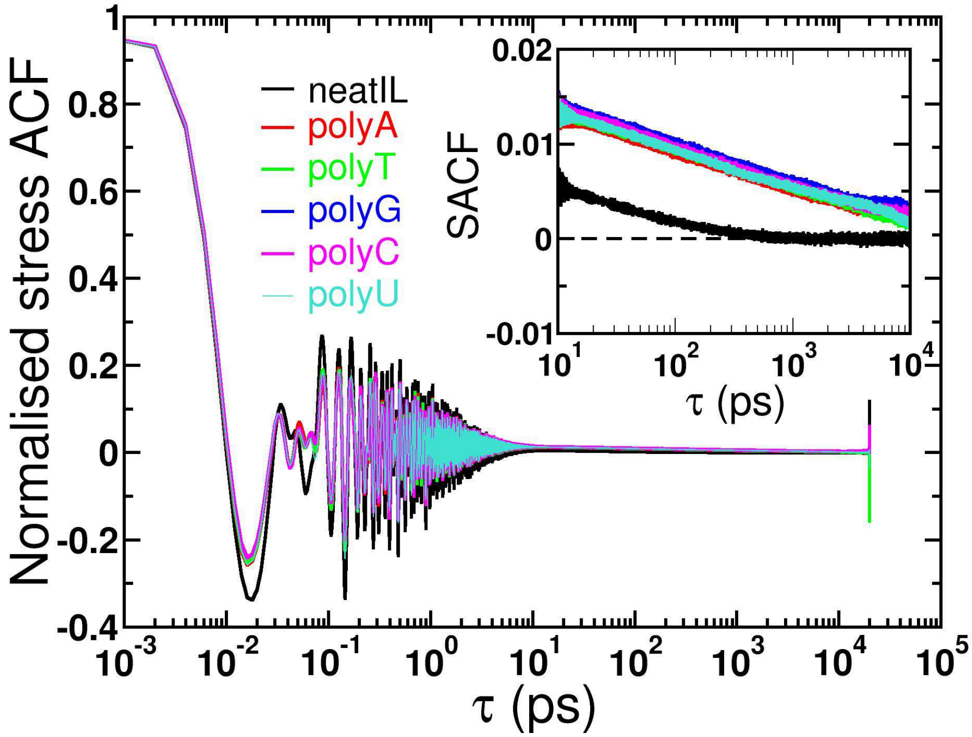

Figure 2 Normalised SACF as a function of correlation time (τ) on a log-log scale. All systems exhibit a characteristic initial decay followed by damped oscillations, indicative of viscoelastic response. Notably, the presence of ssDNA/ssRNA influences the intermediate time behavior, with minor deviations in oscillation amplitude and decay rate compared to neatIL.

Inset: Long-time behavior of the SACF, plotted on a semi-logarithmic scale to highlight persistent correlations. The neatIL (black) shows a more rapid decay than doped systems, suggesting that the biopolymers enhance long-time stress correlations, potentially by modifying the local structuring or dynamic heterogeneity of the ionic liquid environment.

References

[1] W. Humphrey, A. Dalke and K. Schulten, *Journal of Molecular Graphics*, 1996, **14**, 33–38.

[2] H. Tokuda, K. Hayamizu, K. Ishii, M. A. B. H. Susan and M. Watanabe, *J. Phys. Chem. B*, 2004, **108**, 16593–16600.

[3] B. L. Bhargava and S. Balasubramanian, *J. Chem. Phys.*, 2007, **127**, 114510.

[4] R. Galindo-Murillo, J. C. Robertson, M. Zgarbová, J. Šponer, M. Otyepka, P. Jurečka and T. E. Cheatham, III, *J. Chem. Theory Comput.*, 2016, **12**, 4114–4127.

[5] M. Zgarbová, M. Otyepka, J. Šponer, A. Mládek, P. Banáš, T. E. Cheatham and P. Jurečka, *Journal of Chemical Theory and Computation*, 2011, **7**, 2886–2902.

[6] S. V. Sambasivarao and O. Acevedo, *Journal of Chemical Theory and Computation*, 2009, **5**, 1038–1050.

[7] D. A. Case, T. E. Cheatham, T. Darden, H. Gohlke, R. Luo, K. M. Merz, A. Onufriev, C. Simmerling, B. Wang and R. J. Woods, *Journal of Computational Chemistry*, 2005, **26**, 1668–1688.

[8] L. Martínez, R. Andrade, E. G. Birgin and J. M. Martínez, *Journal of Computational Chemistry*, 2009, **30**, 2157–2164.

[9] A. W. Sousa da Silva and W. F. Vranken, *BMC Research Notes*, 2012, **5**, year.